Available online at www.CivileJournal.org

Civil Engineering Journal

(E-ISSN: 2476-3055; ISSN: 2676-6957)

Vol. 9, No. 03, March, 2023

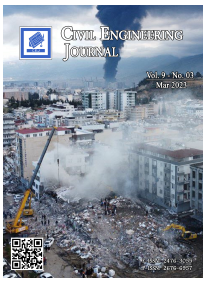

Structural Behavior of Steel Reinforced Concrete Joint Under Flexural Loads

Mohammad M. Handhal [1*], Ali W. Abdulghani [2], Montaqa M. Al-Haydary [3]

[1] *Department of Civil Engineering, College of Engineering, University of Misan, Maysan, 62001, Iraq.*

[2] *Building & Construction Dept, Southern Technical University, Engineering Technical College of Missan, Maysan,62001, Iraq.*

[3] *Architectural Engineering Department, University of Mustansiriyah, Baghdad, Iraq.*

Received 24 November 2022; Revised 07 January 2023; Accepted 19 February 2023; Published 01 March 2023

Abstract

This research investigates the behavior of RC beam column joints reinforced with steel sections. The study deals with the strengthening of RC joints by different steel sections. The investigation included a theoretical analysis through a performing of simulation of beam-column joints laced with steel sections by using FEA. Implementation of the parametric study included reinforcing the concrete beam with steel sections in many configurations. Shapes and length were the most variables in this study, and many shapes were used, such as I-section, box section, and plates, beside the concrete compressive strength variable. The most recent study revealed the possibility of the method to enhance the efficiency of the joint in resisting the loads while the offering many additional features such as higher ductility, stiffness, and energy absorption. The results showed that strengthening by the steel section enhanced the flexural strength of the joint, but these enhancements were to a certain limit due to the concrete strength limitation. The ultimate strength enhancement was 49%, which is considered a good index for the joint efficiency. The use of compressive strength in small amounts led to the enhancements being limited due to the weakness of the concrete. Strengthening the flexural side of the beam by adding a steel section requires stronger concrete to provide more contribution for the steel section to resist more flexural loads. The increase in the compressive strength of the concrete made the improvements reach their peaks. Strengthening by I-shaped and box steel sections showed that the enhancement due to the existence of the I section was greater than that of the box one.

Keywords: Flat Slab; Steel Fibers; Displacement; Ductility; Energy Absorption.

1. Introduction

Beam column reinforced steel joints (BCS) are structural members consisting of reinforced concrete joints with a steel section embedded inside the beam, which is considered a new structural solution for strengthening techniques. The weak point in the member is the joint when subjected to a load. The presence of the steel reinforcement will provide energy absorption to the joint and prevent sudden failure. The level of energy absorption and ductility, especially of joints under earthquakes, is the most, and the need for high ductility is urgent due to the need for high deformation capacity. In 1951, the Architectural Japan Institute (AIJ) submitted the most effective regulation [1] regarding steel-reinforced concrete design. In 1967, Furlong [2] investigated the behavior of encased beam-column joints under flexural loads. Then the studies continued till the year of 1973, when Wakabayasi [3] investigated the behavior of reinforced concrete joints in RC buildings subjected to earthquakes. The researcher analyzed ten shapes of steel cross-sections for the beam-column joints in addition to the existence of steel sections. The results revealed that the presence of the steel sections was considered a good replacement for the steel reinforcement, which provided higher ductility than the

* Corresponding author: mohammed_mahood@uomisan.edu.iq

http://dx.doi.org/10.28991/CEJ-2023-09-03-015

conventional steel reinforcement. Mirmiran & Shahawy [4] explored the behavior of confined joints subjected to cyclic loading. The results showed that the cyclic loading degraded the reinforcement capacity, which reduced the ability of the joint to resist the earthquakes. Gioncu & Petcu [5, 6] studied the rotation capacity of double T steel beams and column-beam joints using a local plastic mechanism. To acquire reliable findings, they developed computer software to compute the rotation capacity of beams. In these investigations, continuous steel beams and rigid frames, two different types of construction, both employed standard beams. Different investigations using joint steel-reinforced concrete were carried out by Chen and Lin [7].

The findings demonstrate effective energy dissipation by SRC joints. Giménez-Carbó [8] explored the behavior of RC joints encased in a steel section. The study included performing a literature review. To improve the behavior of reinforced concrete buildings during earthquakes, L-cross-section steel reinforcement is a good option since it increases the element's resistance and ductility. By use of a variable bending movement diagram, Figueirido [9] investigated the behavior of a tubular steel section filled with HSC under a buckling load. Chen et al. [10] analyzed seventeen joints encased in a steel section. The investigation involved concrete and steel sections with multi shapes, such as L and T shapes. The study results revealed that the behavior of the encased joints was comparable to that of Yan et al. [11], who investigated the hysteretic behavior of beam-column joints. Regarding the use of composite materials, Chen and Wu [12] investigated the behavior of the HSC column confined with a steel section, and the results showed that the addition of a steel section provided more ductility to the general behavior and increased the energy absorption capacity. Many countries suffer from the risks of earthquakes, which made it urgent need to strengthen the members with single or composite materials to avoid damage to the buildings. The reinforced concrete structures' behavior, which integrates a steel cross-section, increases the section's flexibility and energy-absorbing ability while shielding the steel structure from fire. Therefore, joint reinforcement is highly helpful whenever there is an earthquake risk since it will massively increase the structure's ductility, especially in facilities like hospitals, schools, conference centers, theaters, and cinemas that should provide more safety when earthquakes strike. Therefore, joint reinforcement is highly helpful whenever there is an earthquake risk since it will massively increase the structure's ductility, especially in facilities like multistorey buildings, schools, hospitals, etc. Steel sections in beam-column joints have the benefit of reducing the amount of reinforcing required for the concrete in the joint, which is typically a challenging structure to construct. Numerous scientific studies on the behavior of joints in steel-reinforced concrete have been conducted recently.

Bossio et al. (2017) [13] presented a theoretically simplified formulation regarding the failure behavior of beam-column joints, which concluded that it is possible to predict the failure behavior of the joints. Shoukry et al. (2022) [14] investigated the behavior of strengthened joints under seismic loads. The study included strengthening the joint externally with steel plates. The results explored that strengthening enhanced the ultimate strength and prevented brittle failure of the joint. Chu et al. [15] et al. studied the seismic behavior of damaged beam column joints strengthened with many techniques. The outcomes revealed that the addition of diagonal bars improved the joint shear strength. The most enhancements occurred in interior joints greater than exterior ones. Ruiz-Pinilla et al. [16] studied the effect of adding external steel rebar to the beam-column joint. The methods of strengthening involved confining the joint zone with horizontal and diagonal steel rebar. The results showed that diagonal rebar enhanced the shear behavior more than horizontal rebar. Shen et al. [17], Ru et al. [18], and Mishra et al. [19] investigated the possibility of strengthening beam-column joints with many strengthening techniques, all of which enhanced the ultimate strength, but these enhancements varied according to the strengthening techniques. The failure mechanism of the beam-column joints can occur in a brittle status in which the failure of one joint causes a gradual collapse of the building, as revealed in Figure 1.

Figure 1. The collapse of the concrete building at the earthquake of Kocaeli in 1999: (a) Joint failure at the collapsed building; (b) Brittle failure of concrete joint [3]

Previous research focused only on the shear behavior of such joints, which gives an insufficient foundation for understanding how these joints withstand flexural loads. This gap made it necessary to investigate an additional method to strengthen the joints by using steel sections, which was missed in previous studies. This study includes an investigation of the failure mode, strength, deflection, ductility, stiffness, and energy absorption of the strengthened connections with multi configurations of steel sections, which provide a good foundation for designers and researchers to increase the efficiency of such members.

2. Research Significance

The flexural behavior of RC members and the bond behavior of corroded rebars were the main topics of earlier research on the consequences of corrosion damage. There is a lack of knowledge on how steel-reinforced joints affect the flexural behavior of RC beams. To evaluate the structural behavior of flexural RC joints laced by steel sections, this work proposes analysis techniques employing finite element modeling. The workflow included the first step, which is identifying the research subject, reaching the final step, which is the conclusion, as seen in Figure 2.

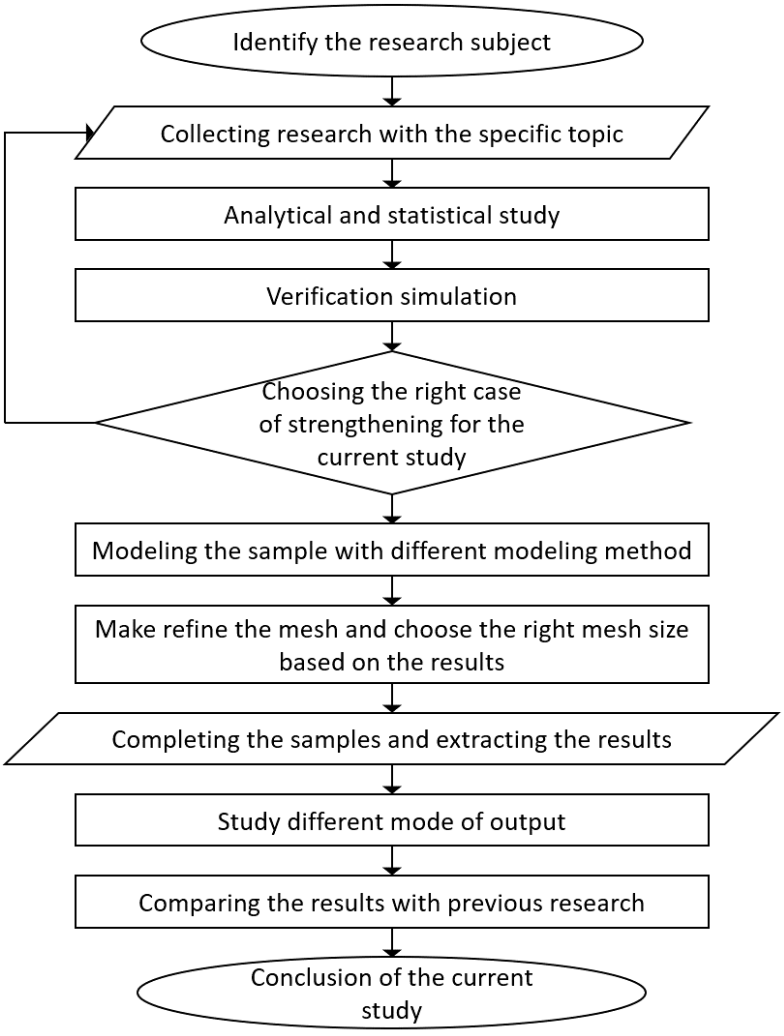

Figure 2. Flow chart of study workflow

3. Finite Element Modeling

Employing the ANSYS program is the most important technique to perform nonlinear analysis for the beam-column joints, and the software deals with the analysis as a finite element. To model the behavior of the beam-column members, the study takes into account the geometry and material nonlinearities. The modeling of joints passes through a series of steps, starting with the modeling and reaching the obtaining of the results. The first step is the pre-processing step, and at this stage the elements were chosen. The selection of the elements must be compatible with the same behavior as the simulated material. The selected elements were SOLID65, LINK180, SOLID185, and SHELL41 to simulate the concrete, steel rebar, steel plate, and steel sections, respectively. The second step was defining the used elements and the behavior of the materials through the real constants and material properties options. This step was used to define the geometrical properties of LINK180 and SHELL41. After that, the stress-strain relationships were used to define the material behavior of all used elements. The later step was the modeling stage, where the models were modeled by the

node-to-node method. This method allows the modeler to control the mesh size of the model to reach peak accuracy in comparison with the experimental results. Applying the loads and supports on the model was the last stage before the analysis, in which the loads were applied to the column in the form of a distributed load on the column. While the supports were simply supported cases. The finite element model has an average element number of 9878, and the column consists of 1773 elements and a beam of 8105 elements. The refined mesh and input values were subjected to a convergence criterion, which revealed non-convergence below 0.2 of the open and close shear transfer coefficients and excellent matching in the number of elements beyond 9000 elements (see Figure 3).

4. Theoretical Work

4.1. Used Elements

The choice of the element is necessary to simulate the structural models, in which the chosen elements must have the same behavior as the simulated materials. In this research, SOLID65 was used to represent the concrete because this element has the same behaviors as the concrete, such as cracking capability, stress, and strain distribution, in addition to the displacement of the node that represents the displacement of the concrete (Table 1). SOLID65 is an element with rectangular faces with eight nodes, and these nodes have three degrees of freedom in the main three global directions (x, y, and Z). It should be noted that the SOLID65 element was so sensitive at the acute angle in the modeling due to the stress concentration phenomenon, which caused crushing with little displacement. Due to the concrete element's (SOLID65) characteristic that considered the failure of any model element to represent the failure of the entire member, the modeling of concrete in this study led the analysis to reach its ultimate load without softening in this load-deflection curve. It should be noted that it is not possible to reach beyond the maximum load if they used SOLID65 for concrete. In this study, SOLID65 was used to represent the concrete material because it offers all the features and behavior of concrete, including the ability to crack and the reactions that match the concrete in reality, which are not available in the steel element (SOLID185). Regarding the steel reinforcement, truss elements (LINK180) were used for the modeling of main and transverse steel reinforcement, which the three-dimensional element has the same behavior as the steel rebar. This element has two nodes, and each node has three degrees of freedom in the main three global directions (x, y, and Z). The LINK180 has elongation capability and stress distribution are identical to those of steel reinforcements. The discrete method was utilized to represent the connection between the steel reinforcement and the concrete, where the concrete and steel rebar were connected through the same node, which provides a perfect bond between the two materials. Concerning the steel section, SHELL41 was utilized to represent the section. This thin element consists of four nodes with a small thickness that can be defined by the real constant. The bearing steel plate was modeled using SOLID185, which consists of eight nodes with three degrees of freedom in each global direction. This element is approximately identical in terms of stress distribution to the steel section, which gave the possibility to use it in the modeling of the steel section [20, 21].

Table 1. Slab's Components details

Material Type	Strength (MPa)	Grade (MPa)
Concrete	25, 45, 55, & 65	-
Rebar Ø10	-	450
Rebar Ø12	-	440
Hooked Fibers	-	1350

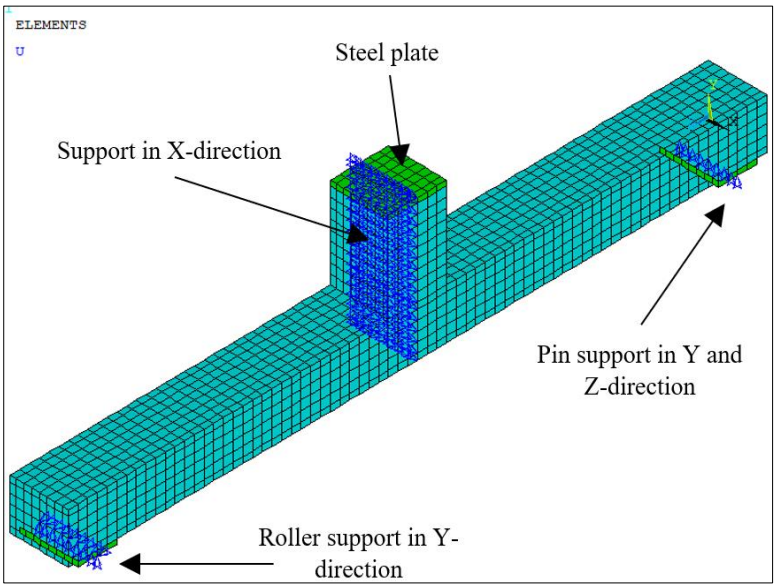

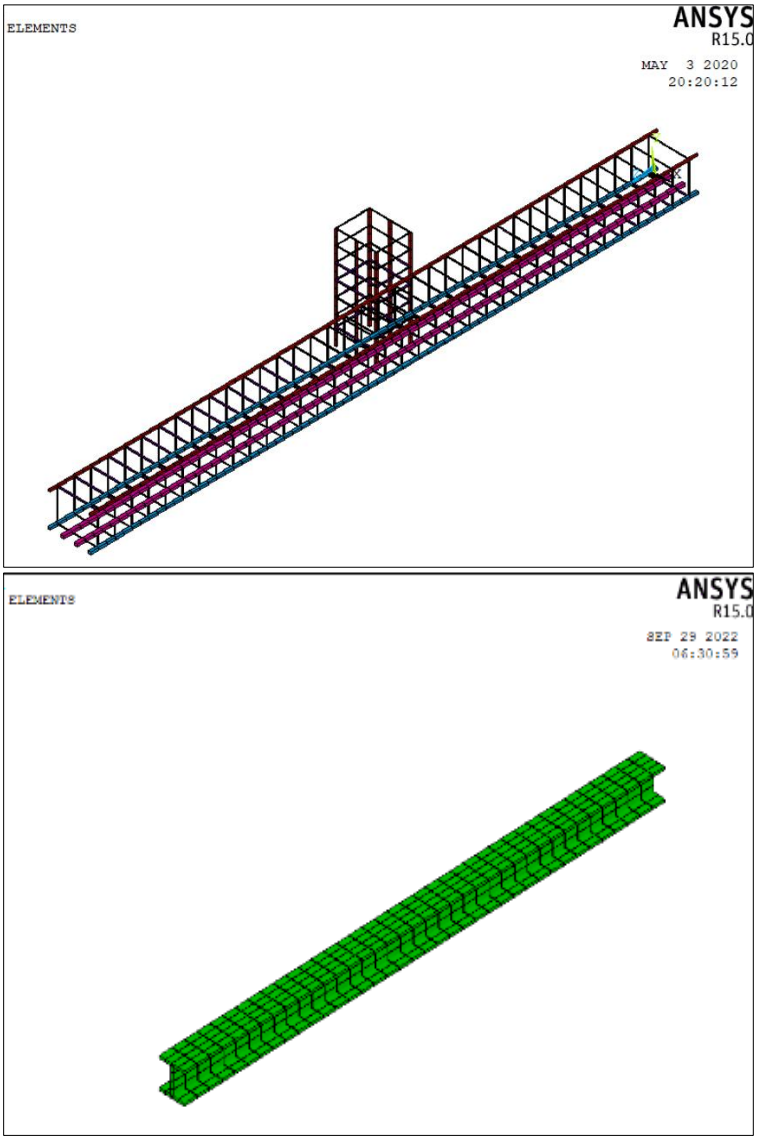

Figure 3. The finite element model shows the mesh and boundary conditions in ANSYS

4.2. Material Behavior

Concrete is an example of a semi-brittle material that behaves differently under tension and compression. Up to roughly 30% of the maximum compressive strength, the stress-strain curve of concrete exhibits linear behavior and is elastic. Then the load continues to increase, reaching the ultimate load, which at this point represents the compressive strength of the concrete ($f'c$). After the ultimate compressive strength (σ_{cu}), the curve drops into the softening region and then failed with obtaining maximum strain (ε_{cu}). Concerning the tension behavior, the curve increases linearly and elastically until it reaches the maximum value of the tensile strength. After this point, the concrete begins to crack and lose strength progressively until it reaches zero [22]. Ultimate uniaxial compressive strength, ultimate uniaxial tensile strength (modulus of rupture), elastic modulus (E), Poisson's ratio (μ), and a reduction factor of stiffness for the cracked tensile condition are essential to define concrete behavior in ANSYS. The constitutive relationship for the concrete, steel reinforcement, steel sections, and steel plates was defined as follows: normal concrete was defined through the equations presented by ACI-318M-19 [23] for the compression and tension. While the HSC is defined according to the equation suggested by Hsu and Hsu [24]. The concrete is defined by a multilinear relationship. Steel reinforcement and sections are defined in ANSYS as a bilinear relationship. The bearing steel plate was modeled and defined as a linear material.

5. Validation

For the verification procedure, three beam-column joints were modeled and compared with an experimental investigation [25]. The computational model utilized in this investigation had the same dimensions, material characteristics, and boundary conditions as the experimental study [19]. The verification revealed extremely high agreement between the experimental and numerical outcomes of the load-deflection curve. Figure 4 showed the possibility of obtaining a convergence in behavior between practical and theoretical studies, provided that all materials are represented in a way that matches their behavior in reality. The verification explored that the plastic strain of concrete

at peak load is the accumulated equivalent plastic strain, indicating the material yields when it is greater than zero. The verification was performed on three joints; two of them were beam-column joints reinforced with steel reinforcement, while the third one was RC joints reinforced with a steel section. The cracking mode of the reinforced joints with steel reinforcement showed that the concrete failed in flexure with vertical cracks developing at the beam bottom surface and extending to the column, as occurred in specimens P03 and P05, as revealed in Figure 4-b. The reinforced steel section joint revealed that the concrete failed in a brittle manner before the yielding of the steel section, which crushed the concrete at the joint zone, which distorted the shear zone. The distortion of the shear zone gave evidence that the concrete in the joints with the laced steel section was the weakest material along the member, which needed to be strengthened by increasing the compressive strength to offer resistance to the steel section.

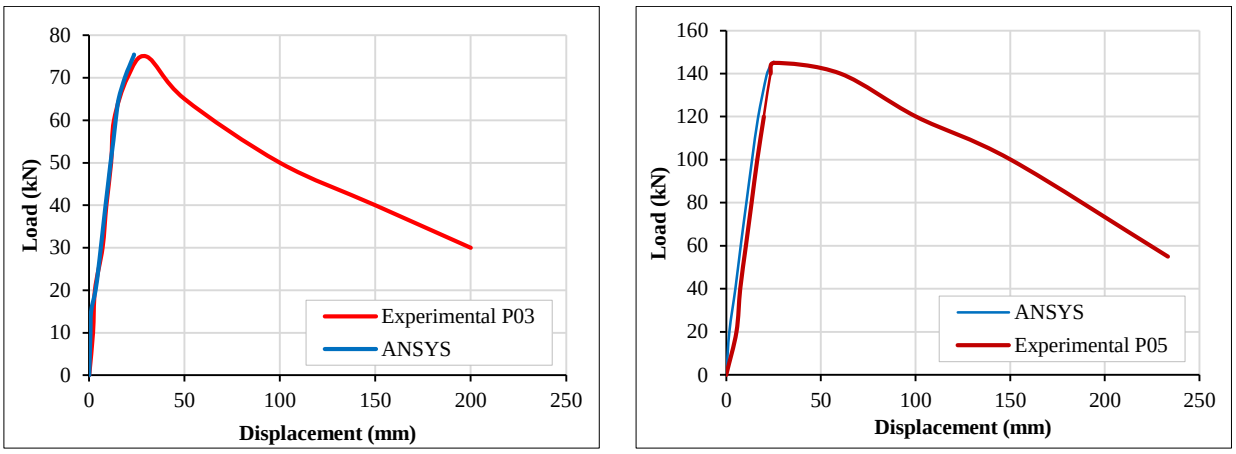

(a)

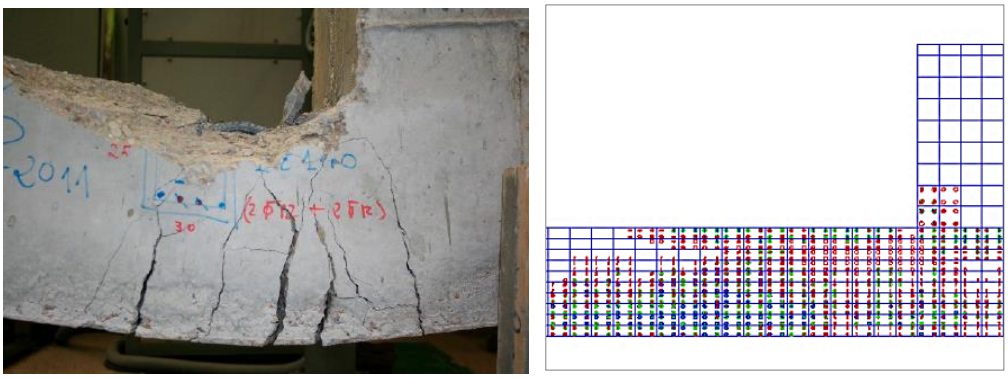

(b)

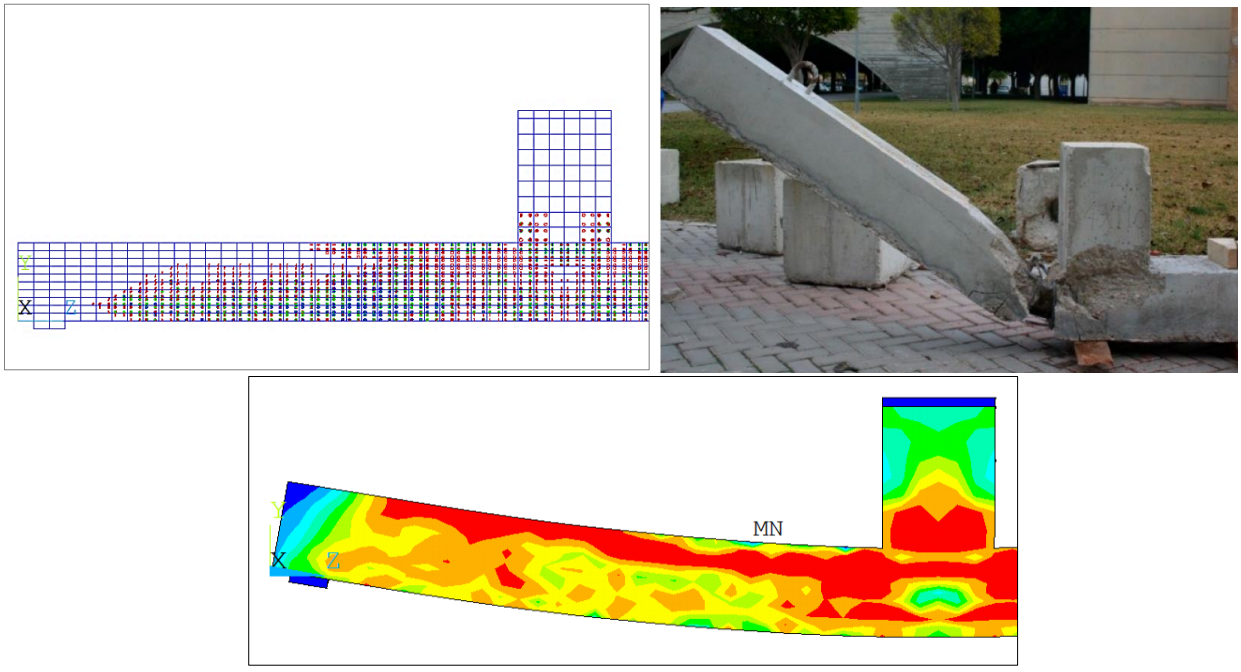

(c)

Figure 4. a) Load-displacement curves clarify the verification work (P03 and P05), b) Crack pattern for the numerical and experimental specimen (P0), c) Crack pattern for the numerical and experimental specimen (P04)

5.1. Theoretical Analysis

Thirteen specimens were performed by various parameters to examine the impact of various factors on the performance of reinforced concrete beam-column joints. The parameters include the use of steel sections in many shapes and lengths. Table 2 and Figure 5 demonstrate the geometric details of the analyzed members. The control joints included reinforcing the beams with four steel rebars of diameter 12 mm at the bottom and two rebars of the same diameter at the top, while the column was reinforced with steel rebar of diameter 16 mm. The transverse reinforcement included the use of 6 mm diameter rebar. Internal strengthening through the use of steel sections is used to enhance the capacity of beam-column joints. These strengthening methods strengthen the full and limited regions of the beam. Regarding the first section series (joint BCJ-I), the beam of the joint was laced with an I steel section (HEB100-S275) with variable lengths (3.5, 2.5, and 1.5 m). The second series of joints included reinforcing the beam in the beam-column joints with box steel sections (#120.5-S275), which were laced at varied lengths (3.5, 2.5, and 1.5 m). The third series included reinforcing the beam with steel plates (10 mm thick). The fourth series included increasing the compressive strength of the steel I-section joints in order to investigate the steel section behaviour.

Table 2. Details of specimens

ID	Compressive strength (MPa)	Steel Section-Length	Parameter
BCJ-RF	25	-	-
BCJ-I	25	HEB100-S275 (3.5 m)	I-Steel sections laced beam
BCJ-I-2	25	HEB100-S275 (2.5 m)	I-Steel sections laced beam
BCJ-I-3	25	HEB100-S275(1.5 m)	I-Steel sections laced beam
BCJ-B	25	#120.5-S275	Box steel section laced beam
BCJ-B-2	25	#120.5-S275	Box steel section laced beam
BCJ-B-3	25	#120.5-S275	Box steel section laced beam
BCJ-HB	25	#120.5-S275	Box steel section laced beam
BCJ-FSP	25	10 mm Thick. Plate	Steel plates laced beam
BCJ-FDP	25	10 mm Thick. Plate	Steel plates laced beam
BCJ-FTP	25	10 mm Thick. Plate	Steel plates laced beam
BCJ-I-45	45	HEB100-S275	Compressive strength
BCJ-I-55	55	HEB100-S275	Compressive strength
BCJ-I-65	65	HEB100-S275	Compressive strength

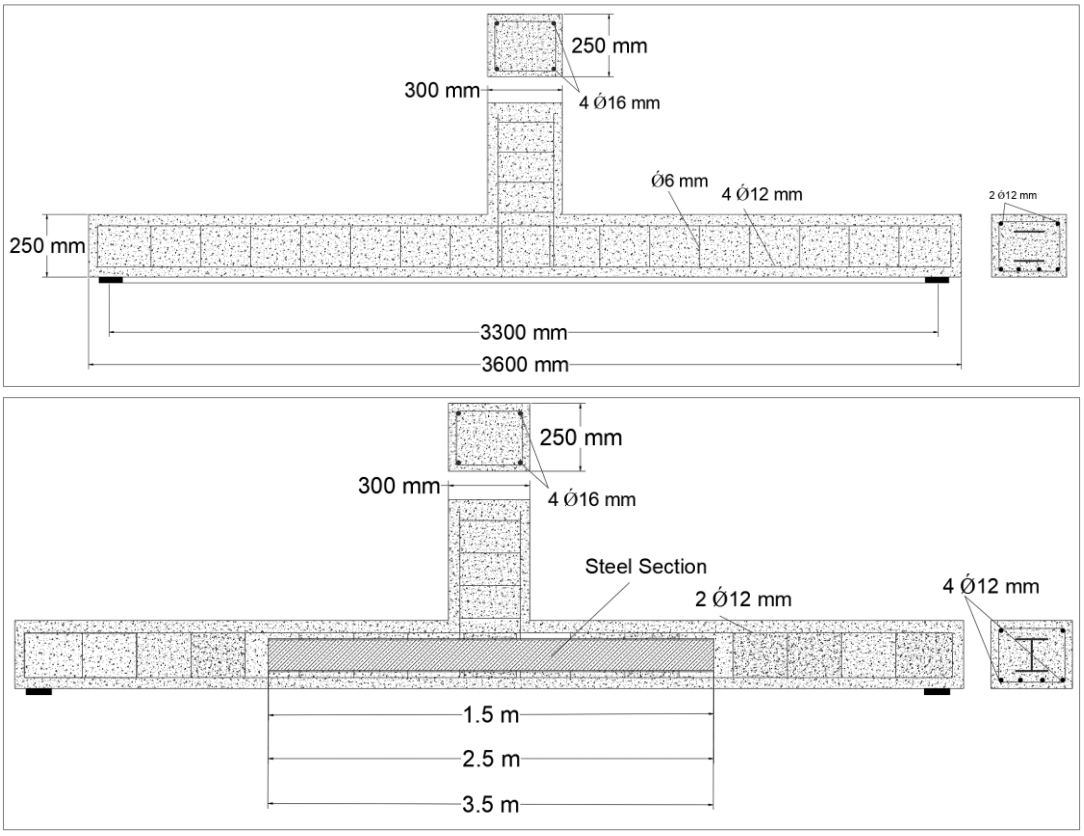

(a) BCJ-RF

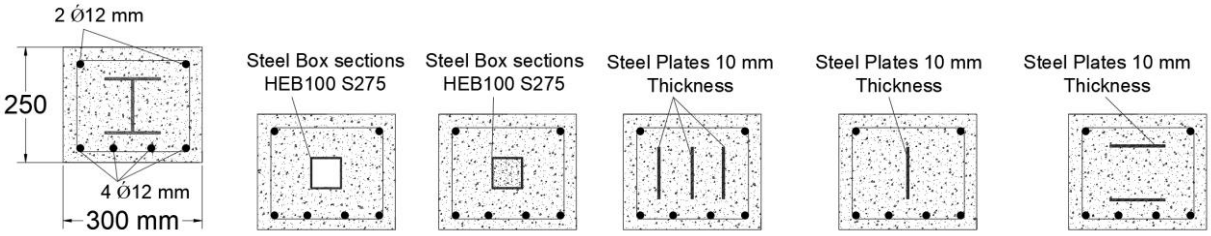

(b) BCJ-I, (c) BCJ-HB (d) BCJ-B (e) BCJ-FTP (f) BCJ-FSP (g) BCJ-FDP.

Figure 5. Elevation view of specimens

5.2. Testing Setup

To achieve the full simulation condition in agreement with the experimental test, the beam-column joint was analyzed and tested as a simply supported beam in which the specimens were supported on the left edge by hinge support, which restrains the specimen for both the horizontal and vertical directions (X and Y directions), while the second side was restrained by a roller, which provided vertical direction restraints (Y direction) (Figure 6). The results were recorded according to the experimental testing, in which the deflection, stresses, and strains were recorded at the same positions as the gauges in the experimental testing. The gauges were distributed in all critical positions (at the positions where the shear and flexural stresses were developed). The load was applied directly on the column over a steel plate to distribute the load over an area and prevent the stress concentration at the column segment.

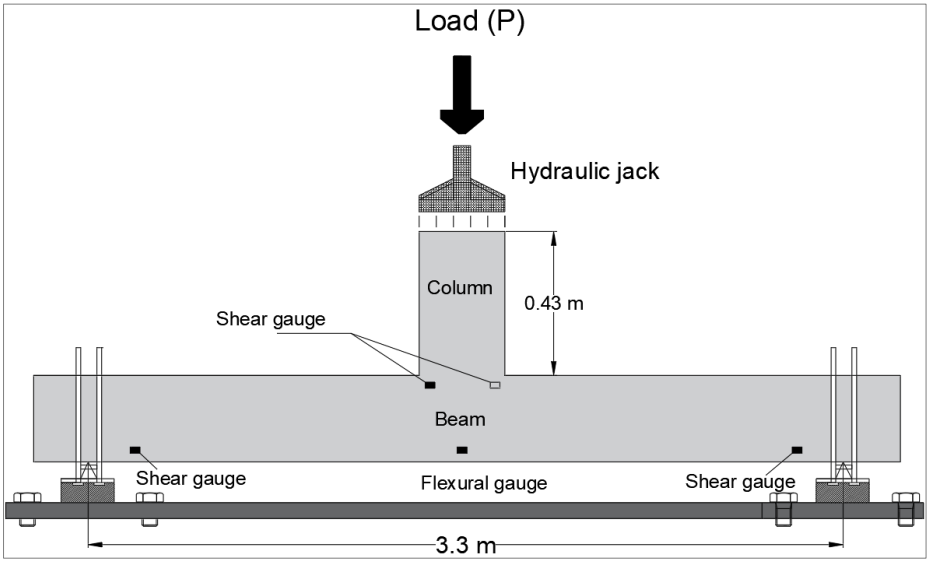

Figure 6. Simply supported testing mechanism

6. Results and Discussion

6.1. Load-displacement Relationship

In this analysis, the control beams' behavior is linearly elastic up to about 34% for control joints (BCJ-RF) and 25.6–46.7% for strengthened joints of the maximum failure load. Overhead this point, the load increases gradually up and reaches the maximum load capacity, as demonstrated in Table 3 and Figure 7. Regarding the effect of steel section shapes, two section shapes were used to strengthen the beam-column joints, which were the I and Box sections. The lacing of the I-section inside the beam showed that the cracking load was enhanced by 31%, the ultimate strength increased by 49%, and the defection decreased by 27.3%, which the existence of the steel section increased the stiffness against loads, as revealed in Figure 7-a. Replacing the I section with a box section showed enhancements in the cracking load and ultimate flexural strength of 8% and 43.2%, respectively, which were less than the improvements than those of I-section model. The deflection decreased at higher values, which were 36.4%, as revealed in Figure 7-b. The length of the resisted section to the flexural loads plays a significant role in the behavior of the beam-column joints. Three lengths of I sections were used for the steel section (1.5 m, 2.5 m, and 3.5 m), which affected directly the behavior of such joints. The variation in the cracking load between the models with three lengths showed increasing the cracking load for the length of 3.5 m higher than that of 1.5 and 2.5 m by 17% and 9%, respectively, as revealed in Table 3.

The ultimate strength increased with the increase of the steel section length by 15.6%, 44.6%, and 49.4% for lengths of 1.5, 2.5, and 3.5 m, respectively, when compared with the reference joint as revealed in Figure 7-b. The deflection increased with the increase in the steel section length, as revealed in Figure 7-b. Regarding the laced box section joint, the increase in length of the steel sections in box shape from 1.5m to 2.5 m and 3.5 m decreased the ultimate strength by a little percentage, but the increase in deflection was by higher percentages, which were 10% and 26.8%, when compared with the joint (BCJ-B) as revealed in Table 3. The use of a hollow box section instead of a filled one decreased the enhancements in ultimate strength from 43% to 29%, as revealed in Figure 7-c. Use of steel plate in three configurations affected the behavior of such joints that use single steel plate (BCJ-FSP), which showed improvements in the cracking load by 5%, 33.7%, and 12.7% when compared with the reference model (BCJ-RF), while the ultimate load carrying capacity increased by 15.6%. The displacement was reduced by 14.2% in comparison with the reference model, as revealed in Figure 7-d. Replacing the single plate with three plates increased the ultimate strength (17.9%) and reduced the displacement by 26.5%, as revealed in Figure 7-d. but use of a double plate in the horizontal direction showed dissimilar behavior in which the cracking load increased by 33.7%, the ultimate load carrying by 37.5%, and the deflection decreased by 26.5%, as revealed in Figure 7-d. In comparison between the obtained results with the results of the previous study [12], it is shown that the enhancements in strength were comparable to those presented by Chen and Wu [12]. The cracking and ultimate load of Chen and Wu [12] got less enhancement than obtained in this study due to the limitation of concrete strength, which the external strengthening reached to its maximum capacity.

Table 3. Results of inverted RCHBs in series one

Beam	Crack load (kN)	Linearity	Failure load (kN)	Maximum deflection (mm)
BCJ-RF	26.14	34.85%	75	24.1
BCJ-I	34.23	30.62%	111.8	17.52
BCJ-I-2	31.3	28.86%	108.44	18.65
BCJ-I-3	28.53	32.91%	86.7	18.81
BCJ-B	28.41	26.46%	107.38	15.33
BCJ-B-2	27.83	26.70%	104.22	16.87
BCJ-B-3	26.42	32.04%	82.45	19.44
BCJ-HB	24.87	25.64%	97	14.06
BCJ-FSP	27.41	31.62%	86.69	20.675
BCJ-FDP	34.95	33.88%	103.16	17.73
BCJ-FTP	29.47	33.33%	88.41	15.55
BCJ-I-45	89.68	38.24%	234.51	33.98
BCJ-I-55	118.19	40.54%	291.53	41.28
BCJ-I-65	151.59	46.70%	324.61	50.6
BCJ-B-45	77.41	35.21%	219.85	43.9
BCJ-B-55	105.82	37.31%	283.62	54.32
BCJ-B-65	120.85	39.44%	306.42	60.23

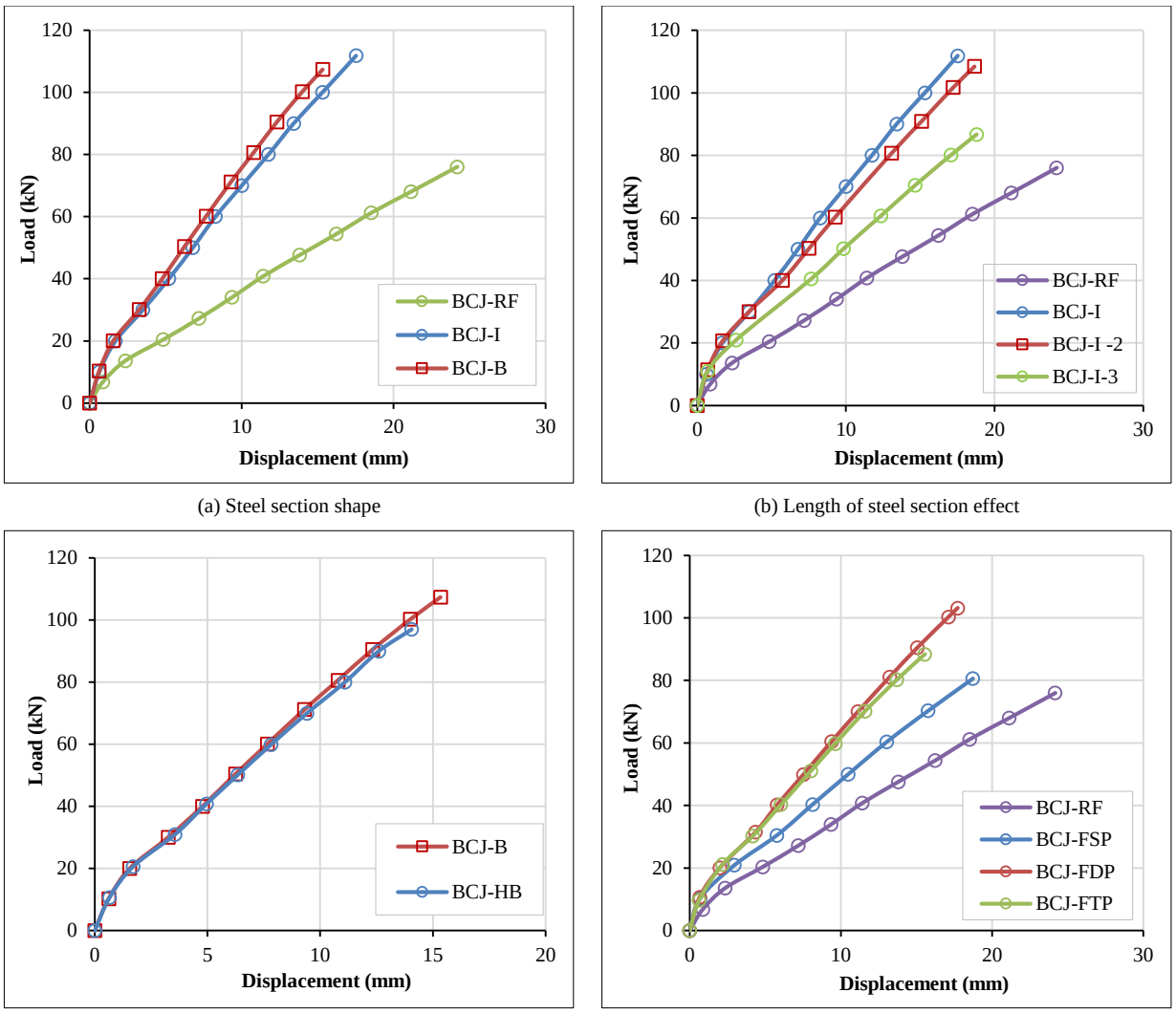

(a) Steel section shape

(b) Length of steel section effect

(c) Bos section variable

(d) Steel plate configuration effect

Figure 7. Load-deflection relationship of the analyzed beam-column joints

6.2. Effect of Compressive Strength

Increase the compressive strength in the range of normal and high strengths to investigate the role of the steel section in resisting the flexural loads. Investigating the effect of the steel section in concrete with 25 MPa led to the enhancements being to certain limits due to the weakness of the concrete. Strengthening the flexural side of the beam by adding a steel section requires stronger concrete to provide more contribution for the steel section to resist more flexural loads. So, the compressive strengths increased to 45, 55, and 65 MPa, respectively. The increase of the compressive strength to 45 MPa for the beam-column joint with an I-section enhanced the cracking and ultimate load carrying capacity by 162% and 109.7%, respectively, when compared with the joint (BCJ-I), as revealed in Figure 8-a. Increasing the compressive strength to 55 and 65 MPa improved the ultimate load by 160.7% and 190.2%, respectively. An increase in the compressive strength caused more deflection at the laced joints, where the stresses propagated along the section. The deflection of the joints increased to 33.98, 41.28, and 50.6, which is equal to more than two times when compared with the control joint, which proved that the steel section cannot reach its peak strength without increasing the compressive strength of the concrete. Regarding the box steel section, the compressive strength increased to 45, 55, and 65 MPa. The increase of the compressive strength to 45 MPa for the beam-column joint with box section enhanced the cracking and ultimate load carrying capacity by 172.4% and 104.7% when compared with the joint (BCJ-B), as revealed in Figure 8-b. Increasing the compressive strength to 55 and 65 MPa improved the ultimate load by 164.1% and 185.4%, respectively. An increase in the compressive strength caused more deflection of the laced joints with box steel sections. The deflection of the joints increased more than those in the I section, which reached 43.9, 54.32, and 60.23, which equates to more than two times when compared with the control joint. Comparing the I-shaped and box steel sections showed that the enhancement due to the existence of the I section was greater than that of the box one, which means that the strengthening role of the I section was greater, but the deflection showed different behavior in that the joints with the box steel section deflected more than those with the I-shaped steel sections.

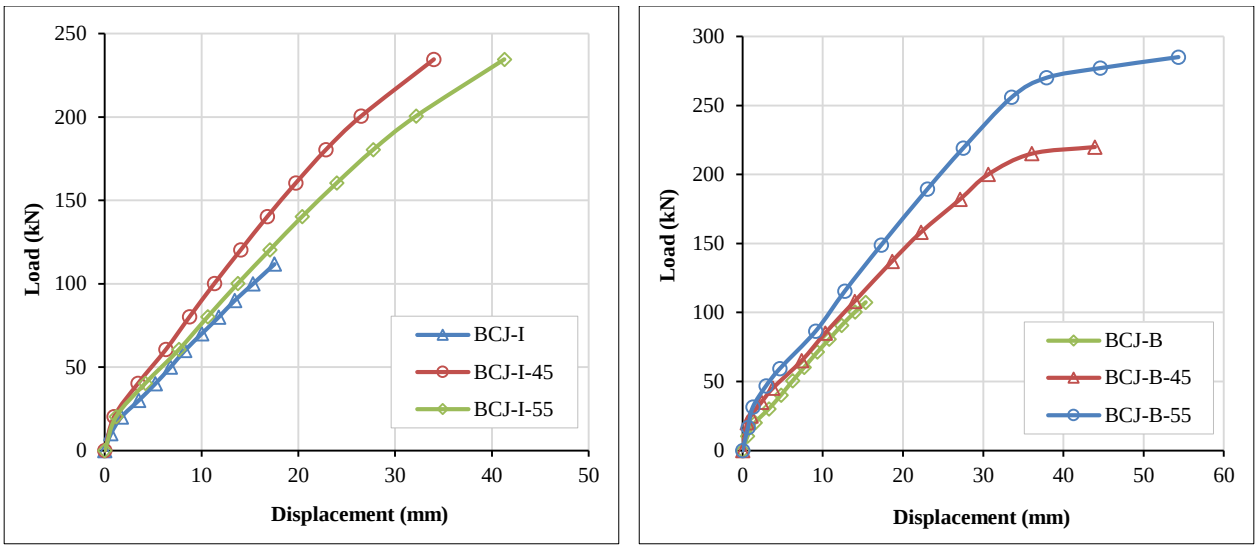

(a) Effect of the compressive strength on Laced I-shaped joints

(b) Effect of the compressive strength on Laced box joints

Figure 8. Load-deflection relationship of the analyzed beam-column joints

6.3. Stiffness

The joint Stiffness represents the concrete's ability to resist deformation against load, as revealed by Baumgart [26]. According to Marzouk and Hussein [27], the stiffness of the joint can be measured by the slope of the elastic stage of the load-deflection curve, which the researchers stated that the stiffness of the concrete is represented by two straight lines with different slopes. The first line represents the uncracked stiffness of the slab (initial stiffness, Ki), and the other represents the post-cracking stiffness (secant stiffness, Ks), as revealed in Figure 9. Initial stiffness is described by the slope of the load-displacement curve reaching up to the first change in the slope (first cracking load), while secant stiffness is defined by the slope of the load-displacement curve extending up to the first yielding of the flexural reinforcement [27]. The presence of the steel sections played a significant role in improving the stiffness of the analyzed joints. Insertion of the I-shaped steel section enhanced the stiffness by 105%, 186.84%, and 148% for the lengths of 1.5, 2.5, and 3.5 m, respectively, as revealed in Table 4. Replacing the I-shaped box sections improved the stiffness more than joints with I-shaped sections. The maximum enhancement in stiffness occurred at the steel sections with 2.5 m length for both shapes, as revealed in Table 4.

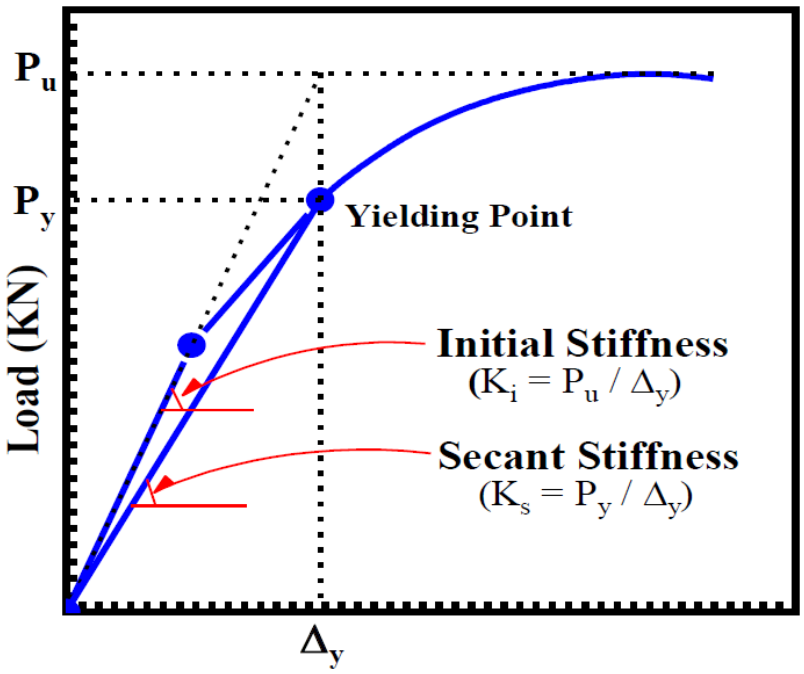

Figure 9. Calculation stiffness

Table 4. Stiffness, ductility, and energy absorption

ID	DI	DI%	K	K%	Tn	Tn%
BCJ-RF	2.87	-	77.80	-	**611.36**	-
BCJ-I	3.27	113.94%	159.53	205.05%	**979.76**	160.26%
BCJ-I-2	3.46	120.56%	145.36	186.84%	1011.31	165.42%
BCJ-I-3	3.04	105.92%	115.23	148.11%	815.03	133.31%
Average		113.47%		180.00%		153.00%
BCJ-B	3.78	131.71%	175.11	225.08%	823.47	134.69%
BCJ-B-2	3.74	130.31%	154.45	198.52%	931.23	152.32%
BCJ-B-3	3.12	108.71%	106.03	136.29%	788.41	128.96%
Average		123.58%		186.63%		138.66%
BCJ-HB	3.90	135.88%	172.48	221.69%	681.92	111.54%
Average		135.88%		221.69%		
BCJ-FSP	3.16	110.10%	104.82	134.73%	896.26	146.60%
BCJ-FDP	2.95	102.79%	145.46	186.97%	914.68	149.61%
BCJ-FTP	3.00	104.53%	142.14	182.70%	687.62	112.47%
Average		105.81%		168.13%		136.23%

6.4. Ductility and Energy Absorption

The presence of the steel parts significantly increased the ductility of the joints. The use of the I-shaped steel section enhanced the ductility by 13.94%, 20.56%, and 5.92% for the lengths of 1.5, 2.5, and 3.5 m, respectively, as revealed in Table 4. Replacing the I-shaped box sections improved the ductility more than joints with I-shaped sections. The maximum enhancement in the ductility occurred at the steel sections with a 2.5 m length for both shapes. Strengthening the joints with steel plates caused little improvement in the ductility, which didn't exceed (4.53%) as revealed in Table 4. Regarding the energy absorption, the most enhancement occurred in the joints laced with I-shaped steel sections, which reached 60.3%, 65.4%, and 33.3% for lengths of 1.5, 2.5, and 3.5 m, respectively, as revealed in Table 4. Replacing the I-shaped box sections decreased the ductility obtained with I-shaped sections, which reached 34.7%, 52.3%, and 28.96% for lengths of 1.5, 2.5, and 3.5 m, respectively. The use of steel plates in multi-configuration showed a median improvement percentage between the I-shaped and box steel sections, as revealed in Table 4. It was determined that the improvements in ductility were equivalent to those given by Chen and Wu [12] after comparing the findings with those of the prior study [12]. Due to the constraint of concrete strength, which the external strengthening attained to its maximum capacity, the ductility load of Chen and Wu [12] received less improvements than those achieved in this work.

7. Crack Pattern and Stress Distribution

The crack patterns of the reinforced joints, as revealed in Figure 10, presented more deformation, which is considered a good index to increase ductility. The crack pattern is affected by the existence of parameters in comparison with the control members, as revealed in Figure 10. The parameters' effectiveness on the crack pattern is clarified as follows; the reference joint showed the appearance of cracks in the flexure zone in a high concentration, which caused the failure at this zone. Also, shear cracks appeared at the connection zone between the column and beam and near the supports. The presence of the steel section caused the appearance of flexural cracks in wide propagations and reduced the appeared shear cracks at the connection region and near the support, as revealed in Figure 10. The stress propagation showed that the stresses along the strengthened joint were distributed along the joint, as revealed in Figure 11. The stresses in the concrete were higher than the stresses in the steel section due to the weakness of the concrete, which causes the concentration of stresses in the concrete. But in case of an increase in the compressive strength of the concrete, the steel section provided higher enhancements, and the stresses were distributed along the member. Comparing the failure mode with Chen and Wu [12] was dissimilar in terms of crack orientations, which this study included strengthening techniques that provided higher ductility than those of Chen and Wu [12].

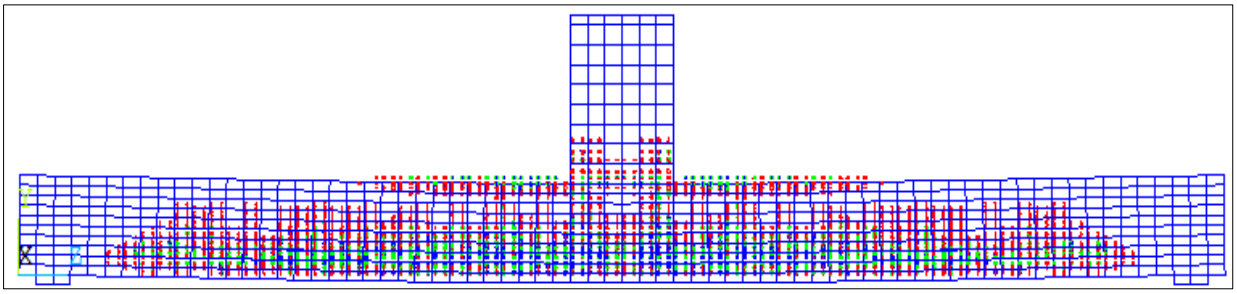

BCJ-RF

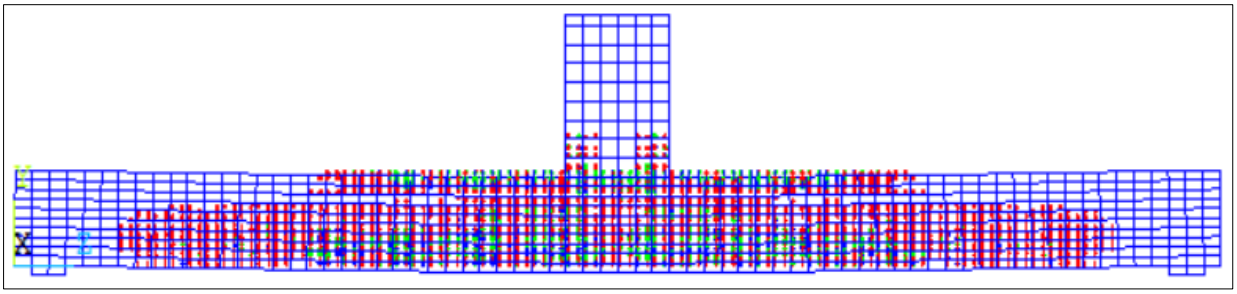

BCJ-I

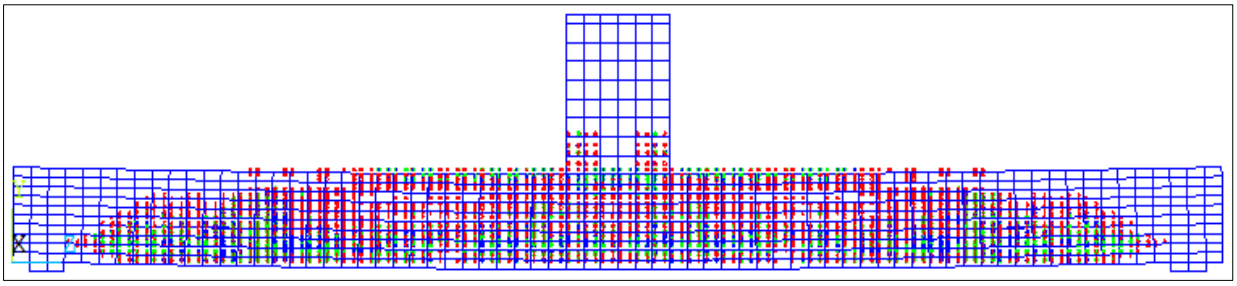

BCJ-I-2

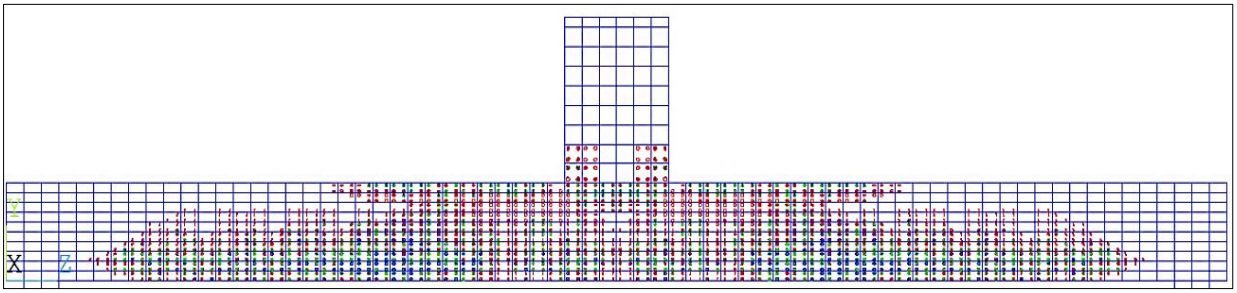

BCJ-I-3

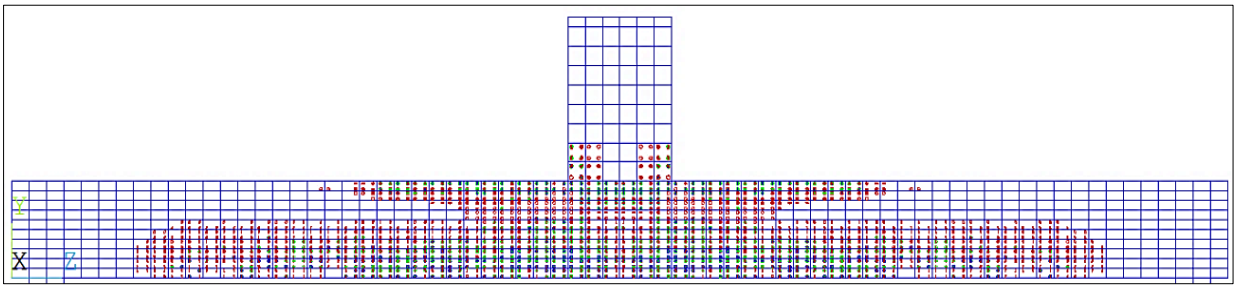

BCJ-B

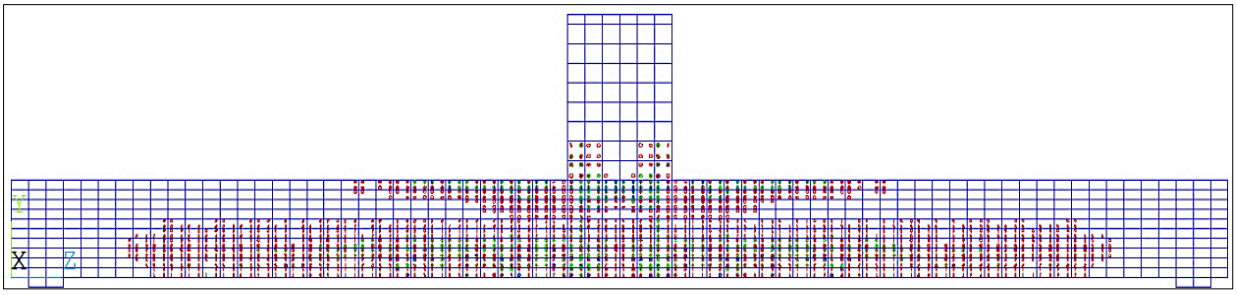

BCJ-HB

Figure 10. Crack pattern and failure mode of analyzed beam-column joints

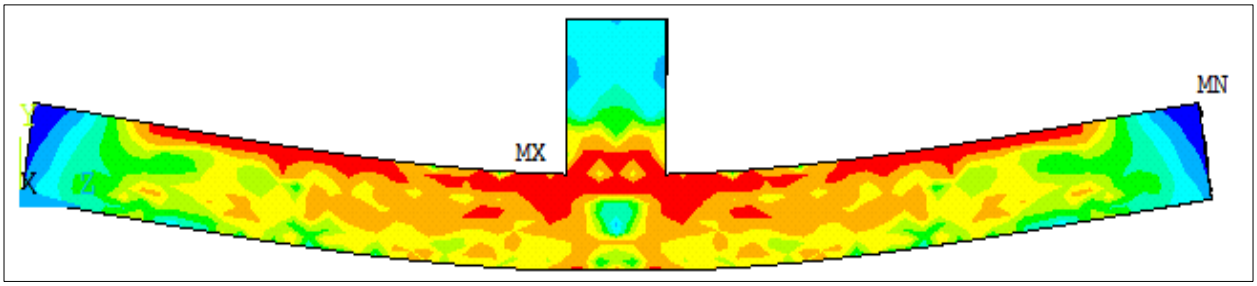

BCJ-RF

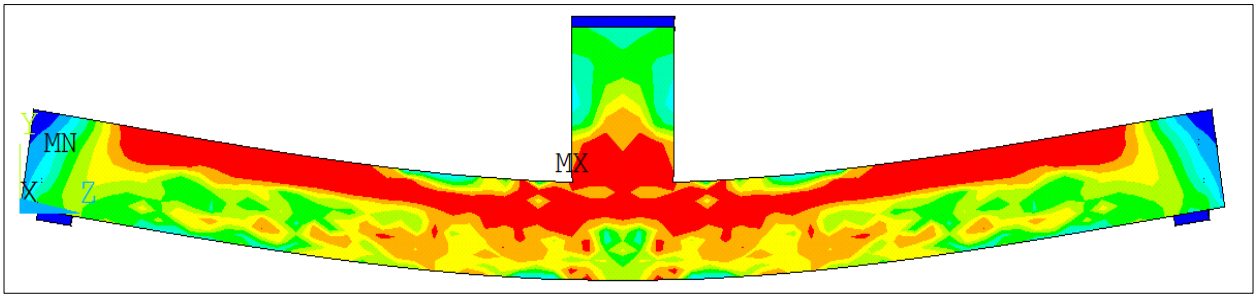

BCJ-I

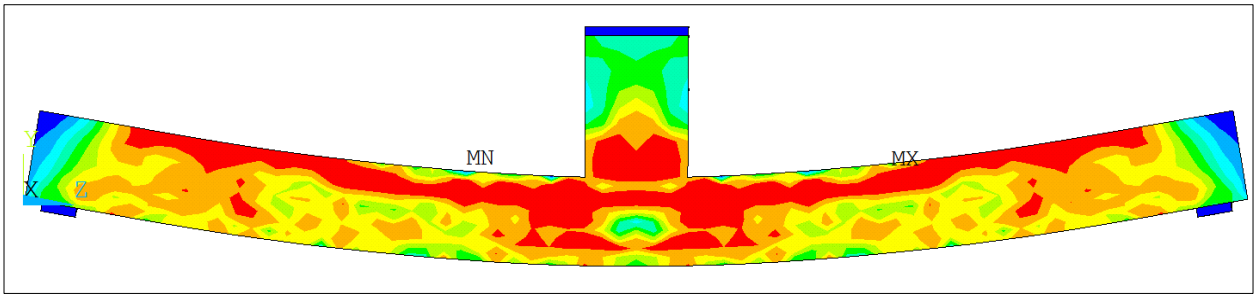

BCJ-I-2

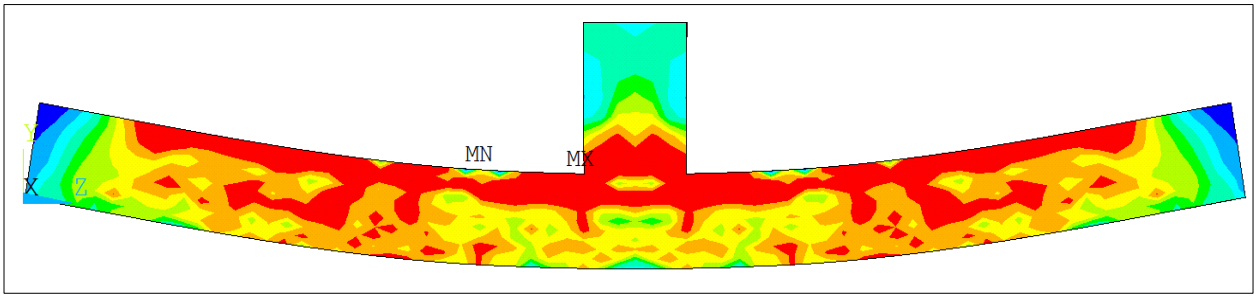

BCJ-I-3

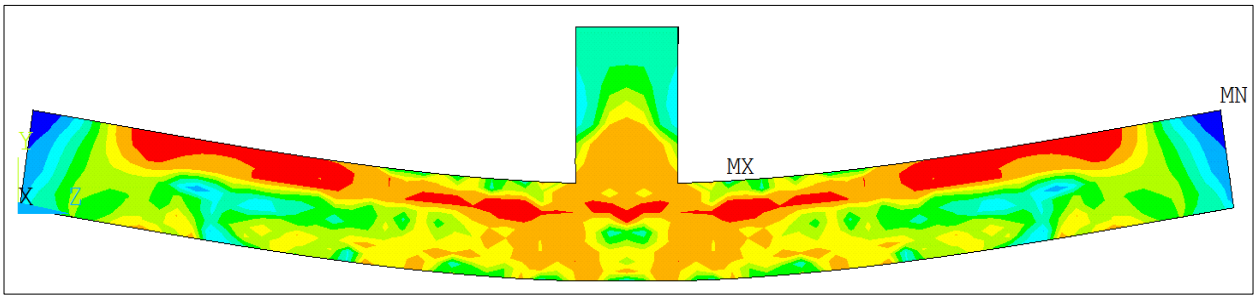

BCJ-B

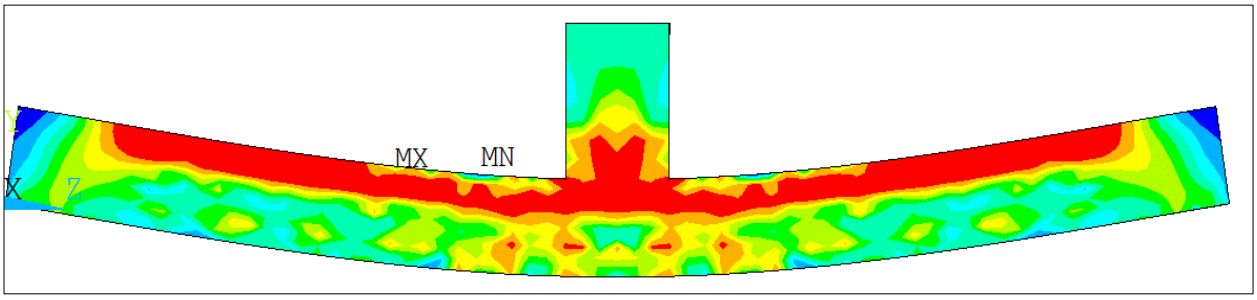

BCJ-HB

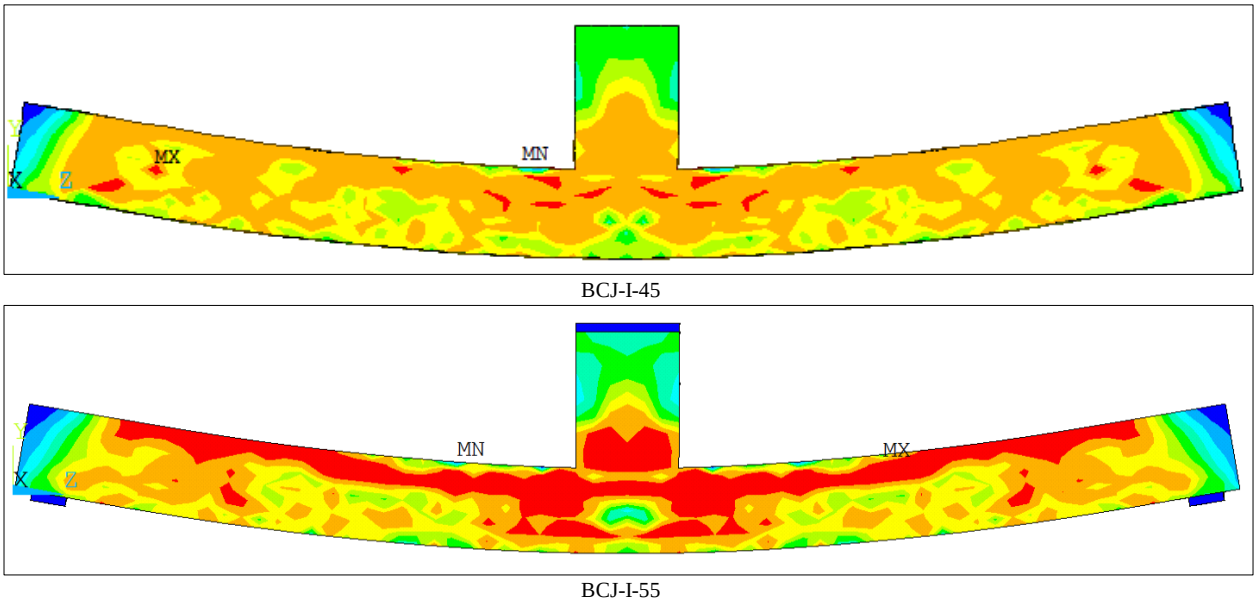

BCJ-I-45

BCJ-I-55

Figure 11. Stress distribution at the failure load of strengthened beam-column joints

8. Conclusions

Engineers typically have to carefully evaluate the flexural behavior of concrete joints laced with steel sections due to the sensitivity of this component in the construction. Visual examinations of concrete joints reinforced with steel may make it difficult to evaluate the true structural performance. So, resorting to the FE was the optimum choice for estimating the remaining capacity and incorporating the effects of the steel section on the behavior of RC joints. The limitation of the application of this strengthening method is the construction cost, which makes this method so efficient at improving the behavior of the joints. Although this method is applicable and recommended for future research. The influence of steel-reinforced beam-column joints on the capacity for strength was ascertained using finite element (FE) analysis, which is now standard for structural engineers and allows for more in-depth assessments. Correlations between analyses and large-scale experimental specimens were analyzed. The present numerical study is focused on the flexural behavior of reinforced concrete beam-column joints in attendance of the parameters. Based on the results obtained from the FEM, it is concluded that how failure occurs varies widely. Many factors have a significant effect on the flexural behavior of joints at failure, and these effects can be summarized as follows:

- The force-displacement graph results obtained for the three models were similar to the experimental tests;
- The strengthened joints by steel sections provided higher deformation capacity. The flexural zone is fully distorted approximately with a large deflection;
- The stress distribution in the joints was redistributed when the use of steel sections exposed less concentration than occurred in the joints without steel reinforcement;
- The behavior showed that the control joints were linearly elastic up to about 34% of the maximum failure load for control joints (BCJ-RF) and 25.6–46.7% for strengthened joints;
- The effect of steel section shapes affected the behavior of the joint, where lacing of the I-section inside the beam showed that the cracking load enhanced by 31%, the ultimate strength increased by 49%, and the defection decreased by 27.3%, but replacing the I-section with a box-section showed enhancements in the cracking load and ultimate flexural strength of 8% and 43.2%, respectively, which were less improvements than those of the I-section model;
- The length of the resisted section to the flexural loads plays a significant role in the behavior of the beam-column joints, which increased the ultimate strength, but the improvement was limited when reaching excessive lengths;
- The use of compressive strengths in the range of 25 MPa led to the enhancements being to certain limits due to the weakness of the concrete. Strengthening the flexural side of the beam by adding a steel section requires stronger concrete to provide more contribution for the steel section to resist more flexural loads;
- Comparing the I-shaped and box steel section showed that the enhancement due to the existence of the I section was more than box one which means that the strengthening role of the I section was more but the deflection showed different behavior which the joints with the box steel section deflected more than the those of I- shaped steel sections;
- The optimum choice of laced section length was 2.5 m, and the increase from 2.5 m to higher lengths increased the ultimate strength with little improvement percentages.

9. Declarations

9.1. Author Contributions

M.M.H., A.W.A., and M.M.A. contributed to the design and implementation of the research, to the analysis of the results and to the writing of the manuscript. All authors have read and agreed to the published version of the manuscript.

9.2. Data Availability Statement

The data presented in this study are available in the article.

9.3. Funding

The authors received no financial support for the research, authorship, and/or publication of this article.

9.4. Conflicts of Interest

The authors declare no conflict of interest.

10. References

[1] AIJ-2014. (2014). AIJ standard for structural calculation of steel reinforced concrete structures. Architectural Institute of Japan, Tokyo, Japan.

[2] Furlong, R. W. (1967). Strength of Steel-Encased Concrete Beam Columns. Journal of the Structural Division, 93(5), 113–124. doi:10.1061/jsdeag.0001761.

[3] Wakabayashi, M. (1986). Design of earthquake-resistant buildings. McGraw-Hill Companies, New York, United States.

[4] Mirmiran, A., & Shahawy, M. (1997). Behavior of Concrete Columns Confined by Fiber Composites. Journal of Structural Engineering, 123(5), 583–590. doi:10.1061/(asce)0733-9445(1997)123:5(583).

[5] Gioncu, V., & Petcu, D. (1997). Available rotation capacity of wide-flange beams and beam-columns Part 1. Theoretical approaches. Journal of Constructional Steel Research, 43(1–3), 161–217. doi:10.1016/s0143-974x(97)00044-8.

[6] Gioncu, V., & Petcu, D. (1997). Available Rotation Capacity of Wide-Flange Beams and Beam-Columns: Part 2. Experimental and Numerical Tests. Journal of Constructional Steel Research, 43(1–3), 219–244. doi:10.1016/S0143-974X(97)00045-X.

[7] Chen, C.-C., & Lin, K.-T. (2009). Behavior and strength of steel reinforced concrete beam–column joints with two-side force inputs. Journal of Constructional Steel Research, 65(3), 641–649. doi:10.1016/j.jcsr.2008.03.010.

[8] Giménez Carbó, E. (2007). Experimental and numerical study of reinforced concrete supports reinforced with metal profiles subjected to simple compression efforts. Ph.D. Thesis, Universidad Politécnica de Valencia, Valencia, Spain. (In Spanish).

[9] Figueirido, D. H. (2012). Experimental study of the buckling of rectangular steel tubular sections, filled with high-strength concrete, under axial load and diagram of variable moments. Ph.D. Thesis, Universidad Politécnica de Valencia, Valencia, Spain. (In Spanish).

[10] Chen, Z., Xu, J., & Xue, J. (2015). Hysteretic behavior of special shaped columns composed of steel and reinforced concrete (SRC). Earthquake Engineering and Engineering Vibration, 14(2), 329–345. doi:10.1007/s11803-015-0026-1.

[11] Yan, C., Yang, D., Ma, Z. J., & Jia, J. (2017). Hysteretic model of SRUHSC column and SRC beam joints considering damage effects. Materials and Structures/Materiaux et Constructions, 50(1), 50. doi:10.1617/s11527-016-0959-5.

[12] Chen, S., & Wu, P. (2017). Analytical model for predicting axial compressive behavior of steel reinforced concrete column. Journal of Constructional Steel Research, 128, 649–660. doi:10.1016/j.jcsr.2016.10.001.

[13] Bossio, A., Fabbrocino, F., Lignola, G. P., Prota, A., & Manfredi, G. (2017). Design oriented model for the assessment of T-shaped beam-column joints in reinforced concrete frames. Buildings, 7(4), 118. doi:10.3390/buildings7040118.

[14] Shoukry, M. E., Tarabia, A. M., & Abdelrahman, M. Z. (2022). Seismic retrofit of deficient exterior RC beam-column joints using steel plates and angles. Alexandria Engineering Journal, 61(4), 3147–3164. doi:10.1016/j.aej.2021.08.048.

[15] Chu, Y., Zhong, Y., Shi, B., & Gong, Y. (2022). Experimental study on seismic performance of seismic-damaged RC frames strengthened by different strengthening methods. Structures, 41, 1475–1487. doi:10.1016/j.istruc.2022.05.103.

[16] Ruiz-Pinilla, J. G., Cladera, A., Pallarés, F. J., Calderón, P. A., & Adam, J. M. (2022). Joint strengthening by external bars on RC beam-column joints. Journal of Building Engineering, 45, 103445. doi:10.1016/j.jobe.2021.103445.

[17] Shen, D., Li, M., Yang, Q., Wen, C., Liu, C., Kang, J., & Cao, X. (2022). Seismic performance of earthquake-damaged corroded reinforced concrete beam-column joints retrofitted with basalt fiber-reinforced polymer sheets. Structure and Infrastructure Engineering, 1–17. doi:10.1080/15732479.2022.2147197.

[18] Ru, Y., He, L., & Jiang, H. (2022). Investigation on a self-centering beam-column joint with tapered steel plate dampers. Journal of Constructional Steel Research, 197, 107479. doi:10.1016/j.jcsr.2022.107479.

[19] Mishra, S., Adhikari, S., & Thapa, D. (2021). Shear capacity and shear reinforcement of exterior beam-column joint of RC building. International Journal of Engineering Research & Technology, 10(3), 335-343.

[20] Jaafer, A. A., & Abdulghani, A. W. (2018). Nonlinear finite element analysis for reinforced concrete haunched beams with opening. IOP Conference Series: Materials Science and Engineering, 454, 012152. doi:10.1088/1757-899x/454/1/012152.

[21] Abdulghani, A. W., & Jaafer, A. A. (2021). Comparative Numerical Study between /Steel Fiber Reinforced Concrete and SIFCON on Beam-Column Joint Behavior. Materials Science Forum, 1021, 138–149. doi:10.4028/www.scientific.net/msf.1021.138.

[22] Legget, R. F. (1964). American society for testing and materials. Nature 203, 565–568. doi:10.1038/203565a0.

[23] ACI 318-19. (2019). Building code requirements for structural concrete (ACI 318-19) and commentary. American Concrete Institute (ACI), Michigan, United States. doi:10.14359/51716937.

[24] Hsu, L. S., & Hsu, C.-T. T. (1994). Complete stress — strain behaviour of high-strength concrete under compression. Magazine of Concrete Research, 46(169), 301–312. doi:10.1680/macr.1994.46.169.301.

[25] Montava, I., Irles, R., Pomares, J. C., & Gonzalez, A. (2019). Experimental study of steel reinforced concrete (SRC) joints. Applied Sciences (Switzerland), 9(8), 1528. doi:10.3390/app9081528.

[26] Baumgart, F. (2000). Stiffness — an unknown world of mechanical science? (2000). Injury, 31, 14–84. doi:10.1016/s0020-1383(00)80040-6.

[27] Marzouk, H., & Hussein, A. (1991). Experimental investigation on the behavior of high-strength concrete slabs. ACI Structural Journal, 88(6), 701–713. doi:10.14359/1261.